# CALCULATIONS AND MEASUREMENTS ON REDUCTION OF THE ENERGY SPREAD AND THE VARIATION IN MEAN ENERGY OF THE 200-MeV LINAC BEAM AT BROOKHAVEN*

K. Batchelor, R. Chasman and N. Fewell
Brookhaven National Laboratory
Upton, New York

## Introduction

During the first year of operation of the 200-MeV injector linac at Brookhaven, it proved desirable to reduce the energy spread and variation in mean energy of 200-MeV without change in current transmission. One way to accomplish this is to maintain the design value of stable phase angle at the input of the machine and to reduce it continuously from there on to the end of the linac. In practice it implies lowering the electric fields in the tanks to maintain the synchronous acceleration for which the machine was designed. The effect is that the available phase acceptance conforms more closely to the longitudinal emittance of the beam and does not grow with energy as in the case of constant synchronous phase.

Computer studies were performed and a "synchronous phase law" was found that combined reduced energy spread and more stable average energy at 200-MeV with unchanged current transmission for beams up to 100 mA. Also, its tolerance requirements with respect to rf phase and amplitude were met by the existing rf system. The computed longitudinal beam parameters of 200-MeV were compared to those calculated for the design fields and a definite improvement was indicated. The fields in the linac tanks were then adjusted accordingly and the output energy spread and mean energy sensitivity to rf phase and amplitude errors were measured and compared to their corresponding values at design field levels.

## Theory

The longitudinal motion in a proton linac is governed by the equation:[1]

$$\frac{1}{\beta_s^3\gamma_s^3}\frac{d}{ds}\left(\beta_s^3\gamma_s^3\frac{d\phi}{ds}\right)+\frac{k_\ell^2}{\sin|\phi_s|}(\cos\phi-\cos\phi_s)=0 \qquad (1)$$

where s is the distance along the machine
$\beta_s c$ = synchronous velocity
$\gamma_s = (1-\beta_s^2)^{-1/2}$
$\phi$ = phase of particle relative to accelerating wave
$\phi_s$ = synchronous phase (<0)

and

$$k_\ell = \left[\frac{2\pi eET\sin|\phi_s|}{\lambda Mc^2\beta_s^3\gamma_s^3}\right]^{1/2}$$

is the wave number for small oscillations. E is the accelerating field amplitude, T is the transient time factor, $\lambda$ the rf wave length and M the proton mass. The deviations of the phase and energy from the synchronous values are given by

$$\Delta\phi=\phi-\phi_s$$

$$\Delta\gamma=\gamma-\gamma_s=-\frac{\lambda}{2\pi}\beta_s^3\gamma_s^3\frac{d\phi}{ds}\ .$$

$\Delta\phi$ and $\Delta\gamma$ are canonical conjugates and the area which a beam occupies in $\Delta\phi$-$\Delta\gamma$ phase space is a constant of motion.

Assuming that $\beta_s$, $\gamma_s$ and $k_\ell$ are constant one can get the longitudinal acceptance at each value of s from the first integral of equation 1:

$$\frac{\pi}{\lambda}\frac{(\Delta\gamma)^2}{\beta_s^3\gamma_s^3}+\frac{eET}{Mc^2}(\sin\phi-\phi\cos\phi_s)=H\ .$$

where $H_{max}$, corresponding to the separatrix or "fish", is given by:

$$H_{max}=\frac{eET}{Mc^2}(-\sin\phi_s+\phi_s\cos\phi_s)\ .$$

The region of stability for $\Delta\phi$ is given by $-\phi_s\le\Delta\phi\le 2\phi_s$ and that for $\Delta\gamma$ by

$$|\Delta\gamma|\le\left[\frac{2\beta_s^3\gamma_s^3eET(\phi_s\cos\phi_s-\sin\phi_s)}{\pi Mc^2}\right]^{+1/2}\ .$$

The acceptance area, A, is proportional to the product $[\Delta\phi_{max}-\Delta\phi_{min}]$ x $[\Delta\gamma_{max}-\Delta\gamma_{min}]$ and hence

$$A\ \propto\left[\frac{2\beta_s^3\gamma_s^3eET(\phi_s\cos\phi_s-\sin\phi_s)}{\pi Mc^2}\right]^{1/2}\cdot|\phi_s|,$$

i.e. for constant machine parameters the acceptance grows as $(\beta_s\gamma_s)^{3/2}$. The dependence of the acceptance on the synchronous phase becomes clear if one writes the constant synchronous acceleration $eET\cos\phi_s=\varepsilon$. One then gets:

$$A\ \propto\left[\frac{2\beta_s^3\gamma_s^3\varepsilon(\phi_s-\mathrm{tg}\phi_s)}{\pi Mc^2}\right]^{1/2}|\phi_s|\ .$$

*Work performed under the auspices of the U.S. Atomic Energy Commission.

In most proton linacs $|\phi_s| \leq 0.60$. Making the approximation

$$\text{tg } \phi_s \approx \phi_s + \frac{\phi_s^3}{3}$$

one obtains

$$A \propto \left[\frac{2\beta_s^3\gamma_s^3\varepsilon}{Mc^2}\right]^{1/2} |\phi_s|^{5/2} .$$

From here one can see that varying $\phi_s$ as $(\beta_s\gamma_s)^{-3/5}$ will keep the acceptance from growing. The area A will remain constant throughout the machine which is necessary in order to maintain the same current transmission as in the case of constant $\phi_s$.

The effect which a varying $\phi_s$ has on the beam parameters can be seen from the solution of equation 1. Assuming that all parameters vary slowly and that $\Delta\phi$ is small one can linearize this equation and get

$$\Delta\phi \approx \Delta\phi_{max} \sin(\int k_\ell ds + \chi)$$

$$\Delta\gamma \approx \Delta\gamma_{max} \cos(\int k_\ell ds + \chi) ,$$

where $\Delta\gamma_{max} = \frac{\lambda}{2\pi}\beta_s^3\gamma_s^3 k_\ell \Delta\phi_{max}$

$\Delta\phi_{max}$ and $\Delta\gamma_{max}$ vary as:

$$\Delta\phi_{max} \simeq \text{const. } k_\ell^{-1/2}(\beta_s\gamma_s)^{-3/2}$$

$$\Delta\phi_{max} \simeq \text{const. } k_\ell^{+1/2}(\beta_s\gamma_s)^{+3/2} .$$

Substituting the expression for $k_\ell$ one obtains:

$$\Delta\phi_{max} \propto (\beta_s\gamma_s)^{-3/4}(\sin|\phi_s|)^{-1/4}$$

$$\Delta\gamma_{max} \propto (\beta_s\gamma_s)^{+3/4}(\sin|\phi_s|)^{+1/4} ,$$

i.e. a reduction of $|\phi_s|$ with s will increase $\Delta\phi_{max}$ and reduce $\Delta\gamma_{max}$ compared to the their values for constant $\phi_s$.

The effects of rf phase and amplitude errors on an initially synchronous particle can be seen from the following: For an amplitude error $\delta E = E\cdot\delta$ and a phase error $\alpha$ the linearized form of equation 1 becomes:

$$\frac{1}{\beta_s^3\gamma_s^3}\frac{d}{ds}\left(\beta_s^3\gamma_s^3\frac{d(\Delta\phi)}{ds}\right)+k_\ell^2\Delta\phi = k_\ell^2[-\alpha(s)+\delta(s)\cot\phi_s] . \quad (2)$$

With $\Delta\phi(s=o)=0$ and $\Delta\gamma(s=o)=0$ the solution to equation 2 is

$$\Delta\phi(s) = k_\ell^{-1/2}(\beta_s\gamma_s)^{-3/2}\left\{\sin(\int k_\ell ds)\cdot \int_0^s k_\ell^{3/2}(\beta_s\gamma_s)^{+3/2}\cos(\int k_\ell ds')\cdot [-\alpha(s')+\delta(s')\cot\phi_s]ds'\right.$$

$$-\cos(\int k_\ell ds)\int_0^s k_\ell^{3/2}(\beta_s\gamma_s)^{3/2}\sin(\int k_\ell ds')\cdot [-\alpha(s')+\delta(s')\cot\phi_s]ds'\Bigg\} .$$

Differentiating and using $\Delta\gamma = -\frac{\lambda}{2\pi}\beta_s^3\gamma_s^3\frac{d\phi}{ds}$ one obtains:

$$\Delta\gamma(s) = -\frac{\lambda}{2\pi}k_\ell^{+1/2}(\beta_s\gamma_s)^{+3/2}\left\{\cos(\int k_\ell ds)\int_0^s k_\ell^{3/2}(\beta_s\gamma_s)^{3/2}\cos(\int k_\ell ds')\,[-\alpha(s')+\delta(s')\cot\phi_s]ds' + \sin\int k_\ell ds\int_0^s k_\ell^{3/2}(\beta_s\gamma_s)^{3/2}\sin(\int k_\ell ds')\,[-\alpha(s')+\delta(s')\cot\phi_s]ds'\right\} .$$

Assuming uncorrelated errors of phase and amplitude in the different tanks and taking averages of the parameters in each tank one gets for the mean square error of the final energy:

$$\left[\Delta\gamma_{av}^f\right]^2 = \left(\frac{\lambda}{2\pi}\right)^2\left(\beta_s^f\gamma_s^f\right)^3 k_\ell^f \sum_i\left(k_\ell^i\right)^3 \left(\beta_s^i\gamma_s^i\right)^3 \left[\langle\delta_i^2\rangle\cot^2\phi_s+\langle\alpha_i^2\rangle\right]\left(\frac{\sin\frac{k_\ell^i l_i}{2}}{\frac{k_\ell^i l_i}{2}}\right)^2 , \quad (3)$$

where the index f refers to values at the output of the linac and i to the $i^{th}$ tank. The summation is over the number of tanks and $l_i$ is the length of the $i^{th}$ tank. It should be noted that for all but the first tanks in a typical proton linac

$$\frac{\sin\frac{k_i l_i}{2}}{\frac{k_i l_i}{2}} \approx 1 ,$$

because the number of longitudinal oscillations per tank is much smaller than one.

From the expression of $[\Delta\gamma_{av}^f]^2$ one can see the effect of a varying $\phi_s$ through the dependence of $k_\ell$ on this parameter. For instance, neglecting a phase factor that was averaged out in equation 3, the contribution to $(\Delta\gamma_{av}^f)^2$ from a phase error in the last tank will be reduced by

$$\left(\frac{\sin|\phi_s^f|}{\sin|\phi_s^o|}\right)^2$$

where $\phi_s^o$ is the initial synchronous phase. In the case of amplitude error the corresponding ratio

will be

$$\left(\frac{\cos\phi_s}{\cos\phi_s}^{f}_{o}\right)^2$$

Noting that

$$\frac{\cos\phi_s}{\cos\phi_s}^{f}_{o} \approx 1$$

in a typical linac an all over improvement in average energy stability should be expected for a decreasing synchronous phase, provided that non-linearities remain small.

## Computer Calculations

All computations were done with a standard longitudinal motion code (LONMO). Machine parameters are those of the Brookhaven linac.[2] Some runs included the effect of space charge, for which a model was used that assumed that the beam was cylindrically symmetric. The beam radius as function of distance along the machine was taken from profile measurements between tanks. The charge density was varied longitudinally only and the beam was represented as a succession of thin discs, each uniformly charged.

In order to find a suitable "synchronous phase law" computer runs were made in the following way:

It was assumed that no buncher was used and that the input distribution consisted of particles distributed uniformly in the region $-\phi_s \leq \Delta\phi \leq 2\phi_s$ and with zero energy spread. (For constant synchronous phase such a distribution is fully transmitted through the linac.) Space charge forces were neglected. The synchronous phase was varied as $(\beta_s\gamma_s)^{-3/5}$ with a small correction accounting for the fact that the synchronous acceleration $\varepsilon$ varies slightly in the Brookhaven linac. A run through the linac showed that some beam losses occur under these conditions.

The run was then repeated with $|\phi_s| \propto (\beta_s\gamma_s)^{-1/2}$ for which full transmission was achieved. With this law $|\phi_s|$ is reduced from 32° at injection to 8° at 200 MeV. Rms phase and energy spreads were calculated as function of drift tube number and the theoretically predicted reduction in energy spread at 200 MeV was obtained. For a 100mA beam, however, approximately 30% of the beam was lost for this "synchronous phase law". Furthermore, an investigation of the average energy sensitivity for rf phase and amplitude errors showed that even in the zero space charge approximation, rf phase and amplitude errors in tanks 1 through 5, as small as 0.30% in amplitude and 1° in phase, caused small parts of the beam (∿10%) to be lost. Since these errors are the quoted tolerances of the present rf system the $|\phi_s| \propto (\beta\gamma)^{-1/2}$ law had to be abandoned even for low intensity beams.

Because the beam losses were largest for phase and amplitude errors in the early part of the linac, it was decided to try a "synchronous phase law" for which the value of $|\phi_s|$ varied from 32° at injection to 8° at 200 MeV but which varied linearly with drift tube number between these two values. $|\phi_s|$ and the corresponding field levels are shown in figure 1. The $|\phi_s| \propto (\beta\gamma)^{-1/2}$ law is also indicated in this figure for comparison. Satisfactory results were obtained from computer runs with the linear phase law. 100% transmission was obtained for beam currents up to 100 mA and for rf phase and amplitude errors which were more than five times larger than the quoted tolerances of the linac rf system.

Results from computer runs with the linear phase law are shown in Fig. 2-5 and compared to those obtained for constant synchronous phase.

Fig. 2 shows single particle phase oscillations and demonstrates the reduction of number of longitudnial oscillations in the case of variable synchronous phase. In Fig. 3 rms phase and energy spreads are shown as function of drift tube number for low intensity beams. Results shown in Fig. 3c were obtained by additional small adjustments of the phase and field amplitude in tank 2 (-1° phase shift, +2.5% change in the total field level). The amplitude of the energy spread oscillations varies as $(\sin|\phi_s|)^{1/4}$ and is reduced by a factor of ∿1.4 going from $|\phi_s|=32°$ to $|\phi_s|=8°$. The additional adjustment of phase and field level in tank 2 changes the phase of the energy spread oscillations so that the energy spread will be at a minimum at the output of the machine as is shown in Fig. 3c. As can be seen from this figure the rms energy spread at 200 MeV is reduced to 100 keV from 280 keV obtained for constant stable phase angle. The rms phase spread is increased by roughly the same ratio.

In Fig. 4 the run of Fig. 3 is repeated for 100 mA. Again the energy spread at 200 MeV is reduced by a factor of almost three.

Fig. 5 shows results from a run starting out with an elliptical distribution in longitudnial phase space with semiaxis corresponding to 32° and 25 keV. Such a distribution is somewhat similar to the actual distribution obtained with a buncher. An improvement in energy spread by a factor of ∿2 was obtained with these input calculations.

Sensitivity of the average energy at 200 MeV to rf phase and amplitude errors was also calculated for the linear phase law and compared to that of constant stable phase angle. Phase and amplitude errors were introduced in the individual tanks consecutively and each time the average energy of the particle distribution at 200 MeV was calculated. Table 1 shows the computed results together with measured values. The root mean square error of the final energy resulting from uncorrelated phase and amplitude errors of 1° and 0.3% is also calculated.

As can easily be ascertained, the computed values agree fairly well with the analytical predictions of equation 3.

## Tank Set-up and Measurements

The tank levels were first adjusted so that they approximately followed the law shown in Fig. 1. In tank 1 and 2 changes of the field along the axis of the tank were achieved by tank tilting. Later tanks were flat. Here, the prescribed fields did not vary by more than 2% in a single tank and the field levels were adjusted to the theoretical value in the middle of each cavity.

Finer adjustments or rf phase and amplitudes of the individual tanks were performed by the phase-amplitude method.[3] Figures 6 through 10 show the calculated phase-amplitude plots for tanks 1, 2, 3, 5 and 9. Similar plots obtained with constant synchronous phase are also shown for comparison. The operating points are situated in the place where the normal tank level curves (center curves in the figures) reach the design output energy of the tanks. These points will correspond to increasingly larger positive phases going down the machine in the case of variable synchronous phase and they will remain at 0 phase relative to the initial stable phase angle for constant synchronous phase.

After lowering the field levels current transmission was measured. It remained unchanged for beam currents up to 50 mA compared to values obtained with design fields in the tanks.

Linac output average energy changes with rf phase and amplitude in the tanks were measured and are shown in Table 1. However, a careful check of the monitoring method of the rf level in each tank indicated that setting errors as great as 1.5% were possible and measurements for field amplitude changes are, therefore, suspect. Furthermore, a calibration of the bending magnet, used for the energy measurements, by a NMR method indicated that tank 7 could be in error by as much as 5% in amplitude and corresponding phase. Output energy measured in the past for design fields are also shown for comparison in Table 1.

The 200 MeV energy spread was measured using a bending magnet preceeded by a defining slit. Results from measurements taken under different rf phase and amplitude conditions gave full width energy spreads ranging from 0.6 to 1.3 MeV. Even the upper limit of this range, i.e., 1.3 MeV, is smaller by a factor of 2 compared to values that had been measured earlier for design field levels.

## Conclusion

By varying the synchronous phase angle from -32° at injection to -8° at 200 MeV calculated improvements of 2 and better are obtained for energy spread and sensitivity of mean output energy to rf phase and amplitude errors. Measurements done so far indeed indicate improved longitudinal beam performance but better tank set-up procedures are necessary for more accurate confirmation of the calculated values. Furthermore, lower operating fields ease the burden on the rf power system without causing loss in beam transmission. Number of short-term breakdowns in the modulator system has been reduced by an order of magnitude.

## Acknowledgments

The authors are indebted to Prof. R.L. Gluckstern for discussions on the theoretical part of this work and to the entire linac staff for help with the measurements.

## References

1. See, for instance, R.L. Gluckstern IEEE Trans. Nucl. Sci. NS-16, No. 3 (1969) p. 194.
2. G.W. Wheeler, Proc. of the 1970 Linear Accel. Conf., NAL (1970), p. 1.
3. K. Batchelor, et al. Ibid, p. 185.

TABLE I

CHANGE IN OUTPUT MEAN ENERGY FOR 1% AMPLITUDE CHANGE

| | CONSTANT SYNCHRONOUS PHASE | | VARIABLE SYNCHRONOUS PHASE | |
|---|---|---|---|---|
| Tank | Calculated Value (keV) | Measured Value (keV) | Calculated Value (keV) | Measured Value (keV) |
| 1 | -25 | - | 40 | 20 ± 20 |
| 2 | 29 | - | -60 | -18 ± 18 |
| 3 | 47 | - | 80 | +20 ± 20 |
| 4 | 68 | 44 | -50 | - |
| 5 | -149 | -208 | 170 | - |
| 6 | 103 | 80 | -155 | - |
| 7 | 53 | 28 | -140 | - |
| 8 | -177 | -104 | 55 | - |
| 9 | 115 | 220 | 175 | - |

CHANGE IN OUTPUT MEAN ENERGY FOR 1° PHASE CHANGE

| | CONSTANT SYNCHRONOUS PHASE | | VARIABLE SYNCHRONOUS PHASE | |
|---|---|---|---|---|
| Tank | Calculated Value (keV) | Measured Value (keV) | Calculated Value (keV) | Measured Value (keV) |
| 2 | 33 | 34 | -43 | -70 ± 30 |
| 3 | 40 | 42 | 23 | 50 ± 30 |
| 4 | 50 | 81 | -32 | -2 ± 10 |
| 5 | -170 | -212 | 76 | 80 ± 20 |
| 6 | 110 | 158 | -63 | -85 ± 15 |
| 7 | 51 | 12 | -42 | -110 ± 10 |
| 8 | -200 | -185 | 13 | 11 ± 7 |
| 9 | 120 | 123 | 40 | 75 ± 15 |

RMS output energy error for 0.3% amplitude error and 1° phase error:

Constant synchronous phase: 336 keV

Variable synchronous phase: 172 keV

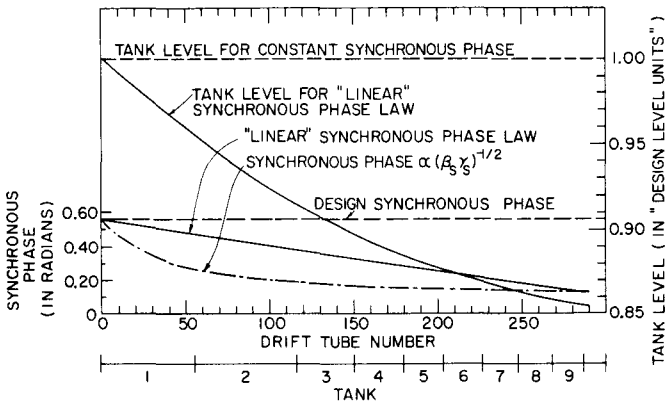


Figure 1. Synchronous phase angle and field level as function of drift-tube number.

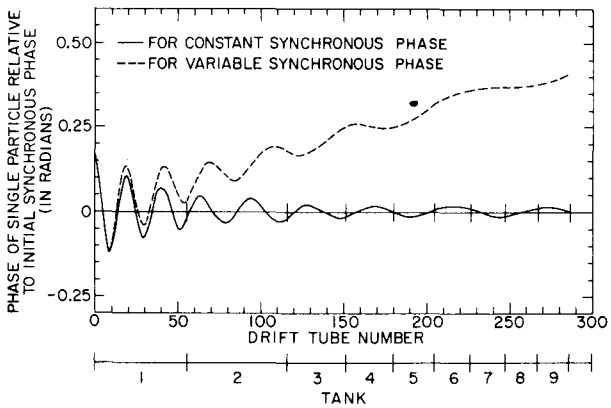


Figure 2. Single particle phase oscillations.

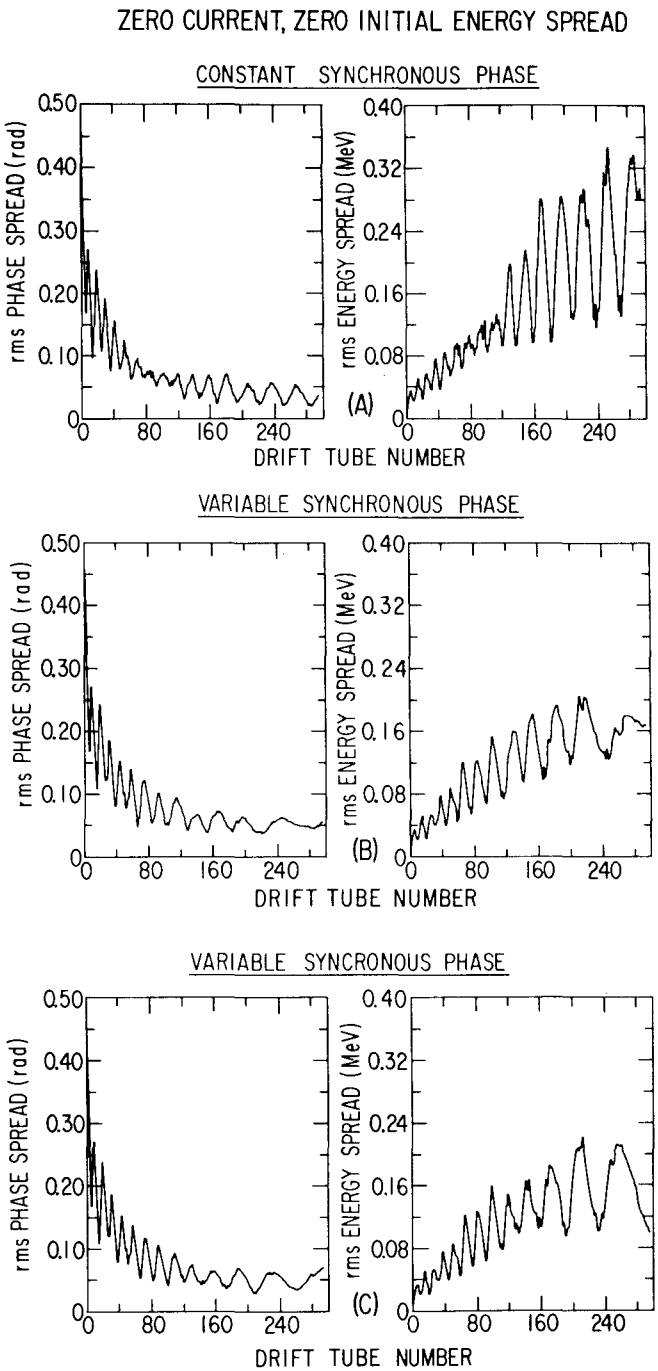


Figure 3. Rms phase and energy spread as function of drift-tube number for zero current and zero initial energy spread.

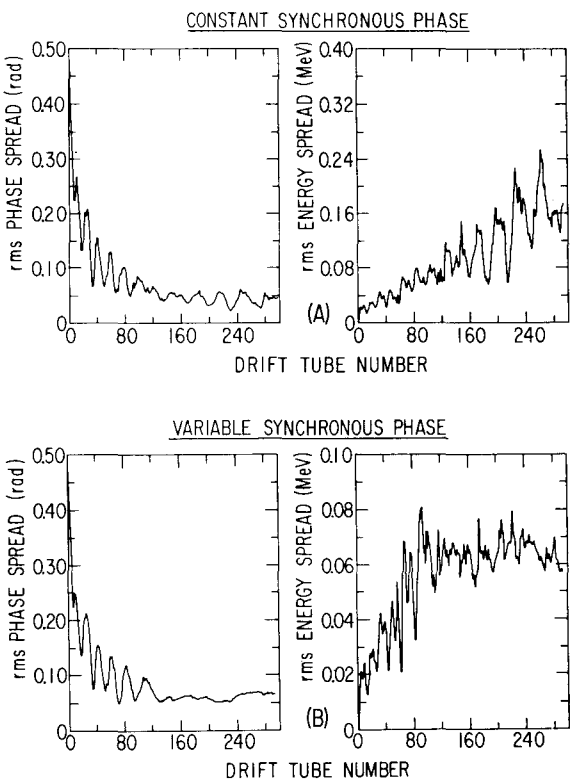


Figure 4. Rms phase and energy spread as function of drift-tube number for 100 mA and zero initial energy spread.

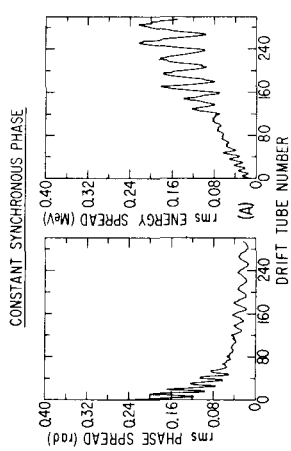


Fig. 5 Rms phase and energy spread as function of drift-tube number for 0 current, ± 25 keV initial energy spread.

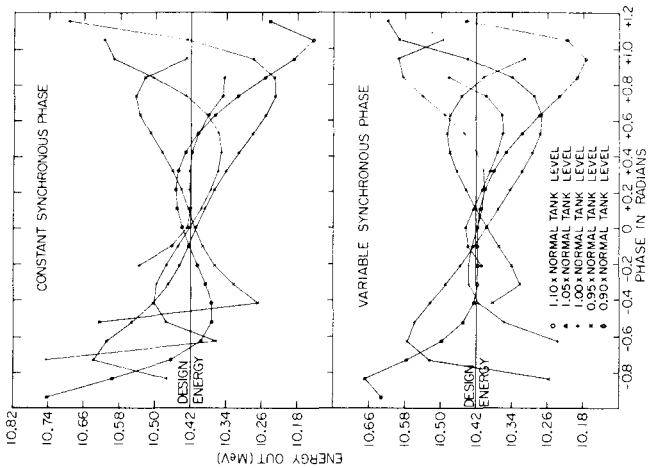


Fig. 6 Phase-amplitude plot for tank 1.

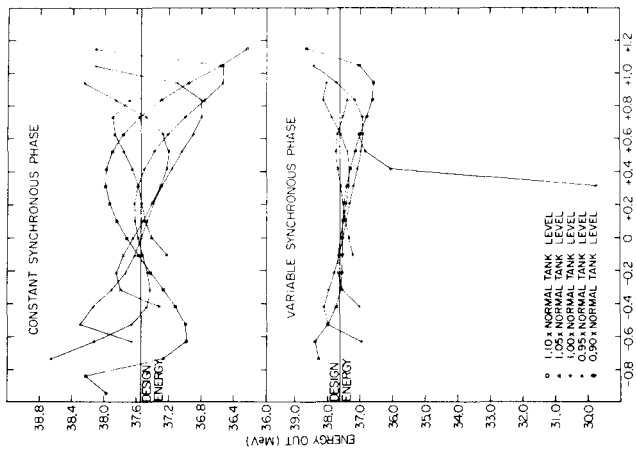


Fig. 7 Phase-amplitude plot for tank 2.

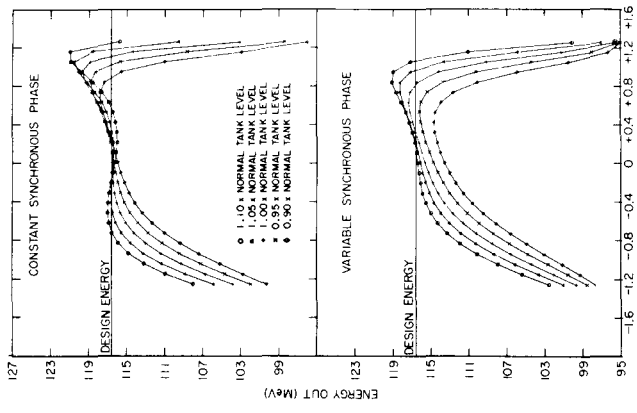


Fig. 9 Phase-amplitude plot for tank 5.

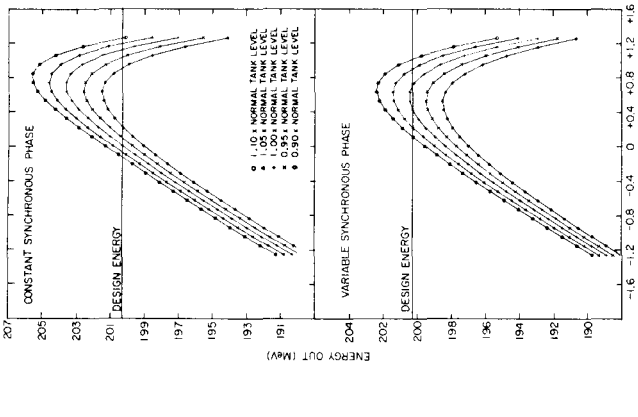


Fig. 8 Phase-amplitude plot for tank 3.

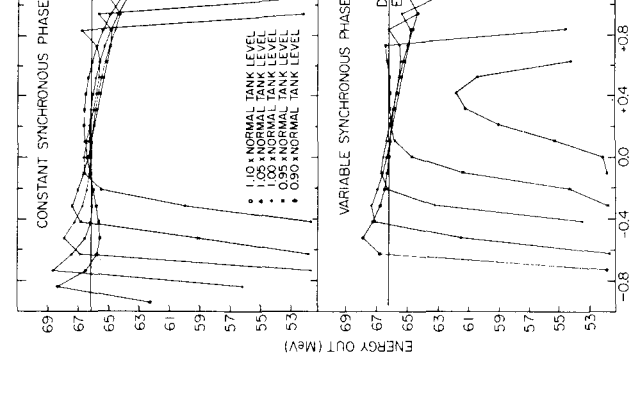


Fig. 10 Phase-amplitude plot for tank 9.